Green's function theory of electrical and thermal transport in single-wall carbon nanotubes

P. J. Lin-Chung, and A. K. Rajagopal
Naval Research Laboratory, Washington, D.C. 20375
(Received 16 July 2001; published 19 February 2002)

The temperature dependencies of electrical conductivity and thermopower are studied for single-wall carbon nanotubes using a Green's-function theory developed to incorporate band structure, dielectric function, and electron-phonon interaction effects. Armchair and zigzag tubes are considered. They exhibit quite different temperature dependencies of the transport coefficients. Some experimental results are compared with the present calculations.

DOI: 10.1103/PhysRevB.65.113408 PACS number(s): 73.63.Fg, 72.80.Rj, 65.80.+n

I. INTRODUCTION

Carbon nanotubes (NT's) have attractive mechanical and electrical properties for applications in electronic devices. Depending on their chiralities, NT's can have intrinsic metallic or semiconducting behavior. The sensitivity of their electronic properties to their geometric structure allows the quantum transports to exist in a very tunable environment.[1] For metallic NT's there are drastic differences compared to common metals in the screening parameters, the Debye temperature, and Fermi energy, which cause weak localization to be observed. For semiconducting NT's the electrical properties can further be modulated through chemical doping or through electrical doping in a field effect transistor (FET) configuration. Existing experimental results for electrical and thermal transport properties of carbon nanotubes exhibit different temperature dependencies for materials prepared in different conditions. Some of the materials studied so far consist of multiwall nanotubes (MWNT's) or ropes and bundles of mixed types of single-wall nanotubes (SWNT's). Thus the analysis of the contribution from individual NT's becomes a formidable task.

Early measurements on MWNT's (Seshadri *et al.*[2]) with tube diameters of about 20 nm (20 walls) show that both the resistivity and the thermoelectric power (TEP) behave similarly to those of graphite.[2] It is possible that these samples contain particles of nanocrystalline graphite during preparation. In addition, interwall electron transport may also modulate the density of states as well as electron-phonon coupling of individual walls.

In the measurements on MWNT bundles performed by Tian *et al.*,[3] the resistance ratio R/R_0 has negative slope in temperature and $\ln T$ dependence below 40 °K, which is attributed to weak-localization effects, whereas the TEP is positive (15 μV/K) and larger than that in highly oriented pyrolytic graphite.

In ropes of SWNT's Hone *et al.* found the TEP to be large and holelike at high T.[4] The measured TEP (50 μV/K) is considerably larger than that of graphite, simple metals, or MWNT's and appears to be an intrinsic property of the SWNT. The temperature dependence of the TEP does not correspond to that of either simple metals, semiconductors, or hopping-type conductivity (power law). Simultaneous existence of hole conduction in metallic NT's and electron conduction in semiconducting NT's has been used to interpret the TEP results.[3,4] The vanishing of the TEP at low temperatures argues against the opening of a gap at the Fermi level, and the upturn of the resistivity at low temperature may be caused by tube-tube interactions in a rope or on-tube defects.

On the other hand, Baxendale, Lim, and Amaratunga found that the TEP is weakly negative in aligned NT's and strongly positive in randomly oriented NT's.[5] Thus the previous observation of positive TEP is attributed not as an intrinsic property but as a consequence of random orientation of intertube contacts relative to the thermal gradient employed in the measurements. However, Collins *et al.*[6] and Hone *et al.*[7] later showed that the TEP is sensitive to the exposure to oxygen and even magnetically aligned SWNT's can have positive TEP when exposed to air.[7]

Theoretical models for conduction in NT's so far include a heterogeneous model at high temperature[8] and variable range hopping models[9] at lower temperature (below 5 K). A comparison between the temperature dependence of the NT and polymer resistivities suggests the heterogeneous model. In this model the heterogeneity is recognized, and the conduction mechanism involves the presence of highly anisotropic good conducting regions separated by ''barrier'' regions. The relative significance of the barriers leads to the crossover of metallic and nonmetallic natures of conduction at a certain temperature T^* without invoking the unrealistic delocalization of carriers or the temperature-induced phase transition. The T^* is found to be sensitive to mechanical handling of samples. The barriers could be interrope or intertube contacts or other defects. However, experiments find that rope-rope contact might increase the resistivity but has little effect on the temperature dependence of the resistivity above 13 K. At low temperature a modest applied electric field is found to completely suppress the upturn in the resistance. This implies that SWNT's are intrinsically metallic, but at low temperature and low electric fields, the charge carriers are localized by disorder and induce an insulating state. Such disorder is likely due to the imperfections in the individual SWNT rather than poor interbundle junctions.[9] Thus a variable range hopping model was proposed for the low-temperature case. Another issue involving conductance in the presence of chemical or electrostatic doping is the charge transfer by doping. The conductance is enhanced by doping, whereas the FET behavior and the oscillations are eliminated by potassium n doping.[10]

In this work we study the temperature dependencies of

electrical conductivity and thermopower for single-wall carbon nanotubes using a Green's-function theory developed to incorporate band structure, dielectric function, and electron-phonon interaction effects in a different context.[11] Armchair and zigzag tubes are considered. In particular, we consider (10, 10) and (18, 0) tubes because these tubes have diameters closer to the narrow diameter range around 1.4 nm observed in the NT ropes.[4,12] Here (n, m) signifies a tube formed by rolling a graphene sheet along the lattice vector $\mathbf{R}=n\mathbf{R}_1+m\mathbf{R}_2$. The purpose of this work is to examine the contributions to the transport coefficients from the electronic structures and electron-phonon interactions for ideal SWNT's. Although it is not possible experimentally to isolate the transport coefficients due to each individual SWNT, at this stage it is of interest to understand their structure dependence in the future design of devices.

II. THEORY

Several techniques have been used in the past to study the transport coefficients. Solving the Boltzmann equation in the relaxation-time approximation by a variational method is the most frequent approach. However, a Green's-function method is often applied for a wider range of scattering strengths. Based on the Green-Kubo-Mori formula, the electrical conductivity σ and thermopower α are given in terms of the correlation functions which are then in turn expressed as Green's functions:[11]

$$\sigma=\frac{2e^2}{\pi\Omega}\int d\omega_2\left(-\frac{dn_f}{d\omega_2}\right)\times\int d\omega\sum_{n,k}[v_n(k)\mathrm{Im}\,G_{nn}(k,\omega_2)]^2\delta[\omega-E_n(k)], \tag{1}$$

$$\sigma\alpha=\sum_{s=1}^{3}(\sigma\alpha)^{(s)}, \tag{2}$$

$$(\sigma\alpha)^{(M)}=(\sigma\alpha)^{(1)}+(\sigma\alpha)^{(2)}=\left(\frac{2\hbar}{\pi\Omega T}\right)\int_{-\infty}^{\infty}d\omega_2\left(\frac{dn_f}{d\omega_2}\right)\omega_2\times\int d\omega\sum_{n,k}[v_n(k)\mathrm{Im}\,G_{nn}(k,\omega_2)]^2\delta[\omega-E_n(k)], \tag{3}$$

$$(\sigma\alpha)^{(2)}=\frac{1}{Td\Omega\hbar}\sum_{q\lambda}\frac{|M_\lambda(q)|^2}{m}\int_{-\infty}^{\infty}\frac{d\omega_2}{2\pi}\omega_2\,\mathrm{Im}\,S(q,\omega_2)\times\left[\frac{\partial^2 n_B}{\partial\omega_2^2}\mathrm{Im}\,D(q,\omega_2)+2\left(\frac{\partial n_B}{\partial\omega_2}\right)\left(\frac{\partial\,\mathrm{Im}\,D(q,\omega_2)}{\partial\omega_2}\right)\right], \tag{4}$$

$$(\sigma\alpha)^{(3)}=\frac{1}{Td\Omega\hbar}\sum_{q\lambda}\frac{q\cdot\nabla_q(\omega_q|M_\lambda(q)|^2)}{m\omega_q}\times\int_{-\infty}^{\infty}\frac{d\omega_2}{2\pi}\omega_2\,\mathrm{Im}\,D_\lambda(q,\omega_2)\times\left[\frac{\partial^2 n_B}{\partial\omega_2^2}\mathrm{Im}\,S(q,\omega_2)+2\left(\frac{\partial n_B}{\partial\omega_2}\right)\left(\frac{\partial\,\mathrm{Im}\,S(q,\omega_2)}{\partial\omega_2}\right)\right]. \tag{5}$$

Here n_f, n_B represent the Fermi and Bose distribution functions, respectively; $E_n(k)$ and $v_n(k)$ in Eqs. (1) and (3) are the energy and velocity of the electron in the nth subband. The conventional notation for the electron-phonon matrix element is used:

$$M_\lambda(q)\equiv W_\lambda(q)\left(\frac{\hbar}{2M\omega_{q\lambda}}\right)^{1/2}, \tag{6}$$

where $W_\lambda(q)$ is the electron-phonon coupling constant.

The electron Green's function, phonon Green's function, and the electron-density-density correlation function are defined as

$$G(k,z)\equiv[z-H]^{-1}, \tag{7}$$

$$D(q,\tau)\equiv-\langle T_\tau[a_{q\lambda}(\tau)+a^+_{-q\lambda}(\tau)][a_{-q\lambda}(0)+a^+_{q\lambda}(0)]\rangle, \tag{8}$$

$$S(q,\tau)\equiv-\langle T_\tau\rho(q,\tau)\rho(-q,0)\rangle. \tag{9}$$

Equation (3) represents the "Mott" term appearing in the Mott formula for metals. After the Matsubara summation, the $\mathrm{Im}\,S(q,\omega)$ in Eqs. (4) and (5) have the form

$$\mathrm{Im}\,S(q,\omega)=\frac{\omega}{\varepsilon(q)^2}\sum_j\int\frac{d^3k}{(2\pi)^3}\int_{-\infty}^{\infty}\left(\frac{d\omega_1}{2\pi}\right)\times G^j(k+q,\omega+\omega_1)G^j(k,\omega_1)\frac{\partial n_f}{\partial\omega_1}. \tag{10}$$

In Eq. (7) the Hamiltonian includes the electron-phonon coupling $(e\text{-}p)$ in fullerene nanotubules, which was discussed by Jishi, Dresselhaus, and Dresselhaus.[13] They found that the interaction of electrons with longitudinal-acoustic phonons gives rise to intraband scattering, and interaction with transverse phonons in the tangential direction gives rise to interband scattering. Experimental measurements on the $e\text{-}p$ interaction in SWNT's found that it is approximately twofold stronger than that in graphite, but approximately 50% smaller than predicted by a tight-binding calculation.[14]

We consider the (10, 10) armchair and the (18, 0) zigzag SWNT's. The electronic structures of these two NT's are quite different. In such SWNT's the $\sigma\text{-}\pi$ mixing, which is proportional to $\sin(\pi/2N)$, with $N=10$ or 18, is negligible. Thus we only consider π bands. In the tight-binding approach the energy dispersions of the mth subbands have the following forms:[15,16]

$$E_m^{(10,10)}(k)=\pm\gamma_0\left[1+4\cos^2\left(\frac{ka}{2}\right)\pm4\cos\left(\frac{m\pi}{10}\right)\right]^{1/2},\quad -\pi<ka<\pi, \tag{11}$$

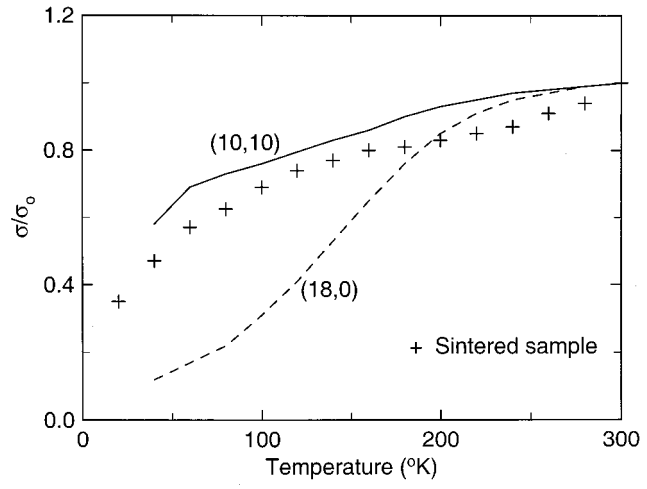

FIG. 1. Calculated electrical conductivity ratio σ/σ_0 as a function of temperature for (10, 10) (solid curve) and (18, 0) (dashed curve) single-wall carbon nanotubes. σ_0 is the conductivity at 300 °K. Data points are experimental measurements from Ref. 4 for sintered samples.

$$E_m^{(18,0)}(k) = \pm\gamma_0\left[1+4\cos^2\left(\frac{m\pi}{18}\right)\pm 4\cos\left(\frac{\sqrt{3}ka}{2}\right)\cos\left(\frac{m\pi}{18}\right)\right]^{1/2},$$
$$-\pi<\sqrt{3}ka<\pi. \qquad (12)$$

For SWNT's we use the value $\gamma_0 = 2.6$ eV for the nearest-neighbor transfer integral.[14] Near the Fermi level, the subband crossing for (10, 10) occurs at $ka = 2\pi/3$ for the 10th subband, whereas the crossing for (18, 0) subbands occurs at $k = 0$.

III. RESULTS

Previous theoretical calculations of electrical conductivity of a graphite layer within a tight-binding framework was found to give $\sigma \sim 13\times 10^5$ ($\Omega\,\mathrm{cm}^{-1}$), which is more than twice that of copper.[17] For NT's, σ is expected to be even greater and highly anisotropic. In the present calculations the electron Green's functions with the e-p coupling are first determined. The integration over the k space is performed using a Monte Carlo method. Our calculated results for conductivity are given in Fig. 1. Some experimental measurements suggest that in a rope the (10, 10) tube tends to have hole-type conduction, and the (18, 0) tube tends to have electron conduction.[3,4] Other measurements suggest electronlike (10, 10) and holelike (18, 0) NT's.[5] We evaluate the relative conductivity σ/σ_0 as a function of temperature for the latter type of conduction in respective tubes. σ_0 denotes the conductivity at 300 °K. In Fig. 1 the experimental data for sintered samples[4] are also shown. Our calculated values for the (10, 10) SWNT are close to the experimental data. The conductivity for (18, 0) deviates from the experimental data especially for lower temperatures. This may indicate that the (10, 10) type of SWNT dominates the sample studied.

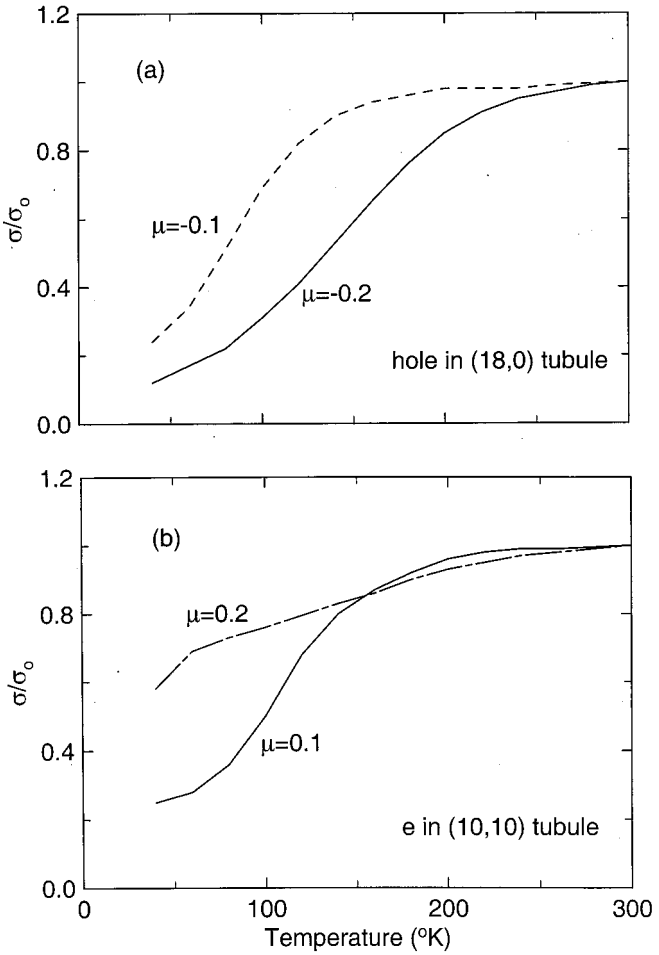

FIG. 2. Calculated temperature variation of electrical conductivity ratio σ/σ_0 at different Fermi levels μ for (a) the (18, 0) and (b) the (10, 10) tubules.

The conductivity ratio in the calculations is found to be sensitive to the position of Fermi energy μ. In Fig. 2 the results for two Fermi energies are displayed. For both types of NT, σ/σ_0 increases sharply with temperature below 150 °K for $|\mu| = 0.1$ eV. For larger Fermi energy, σ/σ_0 approaches 1 more slowly. To our best knowledge, this is the first theoretical evaluation of σ/σ_0 for an individual SWNT.

There have been thermopower measurements on SWNT ropes, mats, pellets, and films, which gave quite different results. The pristine and sintered samples gave thermopower α between 50 and 65 μV/K, at 300 °K, whereas the mat sample gave 40 μV/K.[4] The pellet sample in the experiment of Baxendale, Lim, and Amaratunga has almost zero TEP.[5] The NT bundle has an α less than 20 μV/K,[3] and the magnetically aligned sample gave 27 and 11μV/K, respectively, for annealed and unannealed cases.[7] Unlike the electrical or thermal conductivity, the thermopower is the same when measured perpendicular or parallel to the aligned axis presumably due to the same degree of anisotropy occurring in both thermal and electrical conductivities.[7] Because α involves the interplay of electronic structures and phonon structures, its analysis is more complicated.

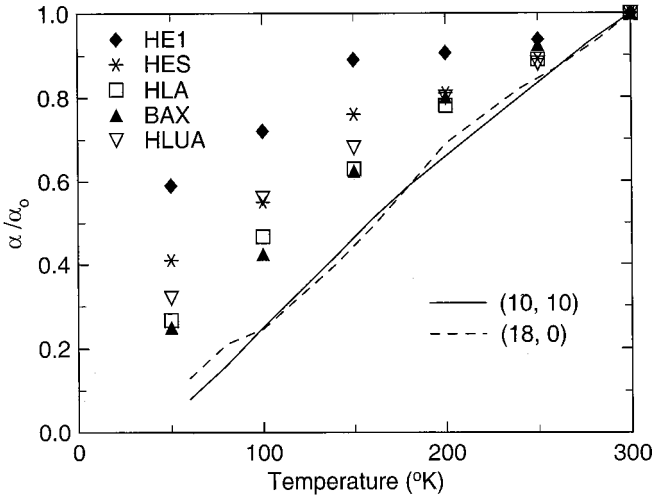

FIG. 3. Calculated temperature variation of thermopower ratio α/α_0 for (10, 10) [solid curve] and (18, 0) [dashed curve] carbon nanotubes. α_0 is the thermopower at room temperature. The experimental data points are obtained from Ref. 4 for SWNT No. 1 sample (HE1) and sintered sample (HES), Ref. 7 for unannealed sample (HLUA) and annealed aligned sample (HLA), and Ref. 5 for SWNT mat (BAX).

Figure 3 displays the calculated thermopower ratio α/α_0 for (10, 10) and (18, 0) SWNT's and the experimental data given in the figure caption. As we can see, the experimental data scatter in a large range. This can be understood by noting that the samples are prepared with widely different conditions as described above. The calculated curves for the armchair and zigzag tubules are similar to each other for the two different types of carrier conduction. From the present calculation, the temperature dependence of α/α_0 for the ideal SWNT is closer to the SWNT mat case in the measurement of Baxendale, Lim, and Amaratunga,[5] than to other measured data. It also confirms that the assignment of carrier-type conduction in metallic and semiconducting NT's seems to be correct. Thus heterogeneity alone is not sufficient to contribute to the scattering of the data points. Defects and variable range hopping may also be responsible.

In contrast to σ/σ_0 in Fig. 1, the α/α_0 vs temperature in Fig. 3 is rather independent of the type of SWNT. This may indicate that the difference in thermal conductivities κ follows the difference in electrical conductivities σ between these two nonchiral carbon fibers as a function of temperature. As a result the thermoelectric properties for these two SWNT's appear to be the same. This is in analogy to the case of observed anisotropies in two transport coefficients σ and κ, and observed isotropy in α of magnetically aligned SWNT films.[7]

In conclusion, the transport properties of SWNT's of armchair and zigzag types are computed using a Green's-function theory of transport coefficients recently developed by us for Si-Ge alloys. Comparison with experimental data shows general trends of TEP as a function of temperature. Our calculation also confirms that the carriers are electronlike in (10, 10) and holelike in (18, 0) NT's. Other type of carriers in these NT's would not give similar temperature dependencies to the experimental data presented here.

ACKNOWLEDGMENTS

The authors are supported in part by the Office of Naval Research.

[1] M. B. Nardelli, Phys. Rev. B **60**, 7828 (1999).
[2] R. Seshadri, H. N. Aiyer, A. Govindaraj, and C. N. R. Rao, Solid State Commun. **91**, 195 (1994).
[3] M. Tian, L. Chen, F. Li, R. Wang, Z. Mao, Y. Zhang, and H. Sekine, J. Appl. Phys. **82**, 3164 (1997).
[4] J. Hone, I. Ellwood, M. Muno, A. Mizel, M. L. Cohen, A. Zettl, A. G. Rinzler, and R. E. Smalley, Phys. Rev. Lett. **80**, 1042 (1998).
[5] M. Baxendale, K. G. Lim, and G. A. J. Amaratunga, Phys. Rev. B **61**, 12 705 (2000).
[6] P. G. Collins, K. Bradley, M. Ishigami, and A. Zettl, Science **287**, 1801 (2000).
[7] J. Hone, M. C. Llaguno, N. M. Nemes, A. T. Johnson, J. E. Fischer, D. A. Walters, M. J. Casavant, J. Schmidt, and R. E. Smalley, Appl. Phys. Lett. **77**, 666 (2000).
[8] A. B. Kaiser, G. Düsberg, and S. Roth, Phys. Rev. B **57**, 1418 (1998).
[9] M. S. Fuhrer, M. L. Cohen, A. Zettl, and V. Crespi, Solid State Commun. **109**, 105 (1999).
[10] R. S. Lee, H. J. Kim, J. E. Fischer, J. Lefebvre, M. Radosavljevic, J. Hone, and A. T. Johnson, Phys. Rev. B **61**, 4526 (2000).
[11] P. J. Lin-Chung and A. K. Rajagopal, Phys. Rev. B **60**, 12 033 (1999).
[12] A. G. Rinzler, J. Liu, H. Dai, P. Nikolaev, C. B. Huffman, F. J. Rodriguez-Macias, P. J. Boul, A. H. Lu, D. Heymann, D. T. Colbert, R. S. Lee, J. E. Fischer, A. M. Rao, P. C. Eklund, and R. E. Smalley, Appl. Phys. A: Mater. Sci. Process. **67**, 29 (1998).
[13] R. A. Jishi, M. S. Dresselhaus, and G. Dresselhaus, Phys. Rev. B **48**, 11 385 (1993).
[14] T. Hertel and G. Moos, Phys. Rev. Lett. **84**, 5002 (2000).
[15] R. Sato, M. Fujita, G. Dresselhaus, and M. S. Dresselhaus, Phys. Rev. B **46**, 1804 (1992).
[16] P. J. Lin-Chung and A. K. Rajagopal, J. Phys.: Condens. Matter **6**, 3697 (1994).
[17] L. Pietronero, S. Strassler, H. R. Zeller, and M. J. Rice, Phys. Rev. B **22**, 904 (1980).